LETTER

An Efficiency-Enhancing Wideband OFDM Dual-Function MIMO Radar-Communication System Design

Yumeng ZHANG[†a)], ***Nonmember***

SUMMARY Integrated Sensing and Communication at terahertz band (ISAC-THz) has been considered as one of the promising technologies for the future 6G. However, in the phase-shifters (PSs) based massive multiple-input-multiple-output (MIMO) hybrid precoding system, due to the ultra-large bandwidth of the terahertz frequency band, the subcarrier channels with different frequencies have different equivalent spatial directions. Therefore, the hybrid beamforming at the transmitter will cause serious beam split problems. In this letter, we propose a dual-function radar communication (DFRC) precoding method by considering recently proposed delay-phase precoding structure for THz massive MIMO. By adding delay phase components between the radio frequency chain and the frequency-independent PSs, the beam is aligned with the target physical direction over the entire bandwidth to reduce the loss caused by beam splitting effect. Furthermore, we employ a hardware structure by using true-time-delayers (TTDs) to realize the concept of frequency-dependent phase shifts. Theoretical analysis and simulation results have shown that it can increase communication performance and make up for the performance loss caused by the dual-function trade-off of communication radar to a certain extent.

key words: *radar-communication, OFDM, precode, beam split, hybrid beamforming*

1. Introduction

Terahertz (THz) dual function radar communication (DFRC) system is a key technology in 5G-Advanced stage research, one of the core visions of 6G. Recently, more attention is focused on DFRC systems with joint DFRC waveform design [1], [2] to guarantee both sensing and communication performance, which is not limited by any existing radar or communication waveforms and is promising to achieve scalable performance trade-off between the two functionalities. For this, spatial modulation techniques that leverage densely packed configurable antenna arrays are investigated to increase capacity and spectral efficiency [3]. Work [4] addresses both radar-centric and joint designs to optimize the DFRC tradeoff waveform by taking into account the feedback overhead of transmitting waveform control information. And [5] considers hybrid beamforming design for orthogonal frequency-division multiplexing (OFDM) DFRC system by jointly optimizing the spectral efficiency (SE) of communication and spatial spectrum matching error (SSME) of radar. However, the above method is only applicable to narrowband systems but not broadband THz systems. Then, a wideband DFRC multiple-input multiple-output (MIMO) OFDM waverform precoding system is jointly designed [6]. But in order to reduce power consumption, the current widely used hybrid beamforming structure can cause beam splitting effect and result in performance degradation. To solve this problem, a delay-phase precoding structure in [7] is used to provide frequency-dependent phase shifts. However, there are seldom researches about improving OFDM-DFRC system performance with hybrid beamforming structure to mitigate the gain loss.

Throughout the letter, hybrid beamforming structure is adopted to reduce power consumption. However, in the THz band design, due to the performance degradation caused by hybrid beamforming, we propose to add time delay components in OFDM-DFRC system to optimize performance. We assume the precoded structure is known, spectrum efficirncy (SE) of the obtained from the known precoded matrix and the expected are compared to derive the communication performance. Also, the spatial spectrum matching error (SSME) between the design spectrum and the expected spectrum is calculated to derive the radar performance. The optimal solution of the precoded structure is obtained by balancing the communication and sensing performance of the DFRC system based on the consensus alternating direction method of multipliers (consensus-ADMM) framework [8]. Furthermore, we use a delay phase precoding method to invert the digital precoding design schemes. In this way, we get a complete MIMO-DFRC precoding design that can be compatible with ideal radar and communication functions, and reduce array gain loss due to beamstrabismus problems caused by broadband.

Notations: unless otherwise specified, lower-case and upper-case boldface letters represent vectors $\mathbf{a}$ and matrices $\mathbf{A}$. $(\cdot)^T$, $(\cdot)^H$ and $(\cdot)^*$ stand for transpose, Hermitian transpose and complex conjugate; $\|\cdot\|$, $\|\cdot\|_\infty$ and $\|\cdot\|_F$ denote the l_2 norm, l_∞ and the Frobenius norm respectively; blkdiag($\mathbf{A}$) denotes a block diagonal matrix where each column of A represents the diagonal blocks of the matrix blkdiag($\mathbf{A}$).

2. System Model

As shown in Fig. 1, we consider a DFRC system, which simultaneously transmits radar probing waveforms to the targets and communication symbols to the downlink users. The joint system is equipped with a uniform linear array (ULA) which has N_t transmit antennas with K true-time-delayers (TTDs), M subcarriers, and N_s serving single-antenna users while detecting radar targets at the same time.

Manuscript received October 21, 2023.
Manuscript revised February 1, 2024.
Manuscript publicized March 4, 2024.
[†]Zhejiang Normal University, China.
a) E-mail: zym1017@zjnu.edu.cn
DOI: 10.1587/transfun.2023EAL2094

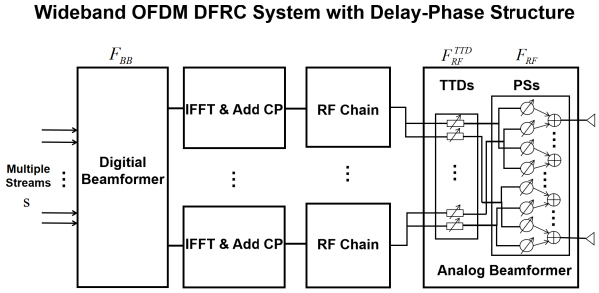

Fig. 1 Overview of a wideband OFDM-DFRC system with delay-phase structure.

2.1 Dual-Functional Precoding Matrix

Assume the dual-functional precoding matrix is known and can be shown as

$$\mathbf{X} = \mathbf{F}_{RF}\mathbf{F}_{RF}^{TTD}\mathbf{F}_{BB}, \tag{1}$$

where the analog beamformer provided by the frequency-independent phase shifters (PSs) with $\mathbf{F}_{RF} = [\mathbf{F}_{RF,1}, \mathbf{F}_{RF,2}, \cdots, \mathbf{F}_{RF,N_{RF}}] \in \mathbb{C}^{N_t \times KN_{RF}}$ and $\mathbf{F}_{RF,l}$=blkdiag $([\bar{\mathbf{f}}_{l,1}, \bar{\mathbf{f}}_{l,2}, \cdots, \bar{\mathbf{f}}_{l,K}])$ denotes the analog beamformer realized by the frequency-independent PSs for the u-th user. The frequency-dependent TTD part satisfies $\mathbf{F}_{RF}^{TTD}$ = blkdiag $([e^{-j2\pi f_m \mathbf{t}_1}, e^{-j2\pi f_m \mathbf{t}_2}, \cdots, e^{-j2\pi f_m \mathbf{t}_{N_{RF}}}]) \in \mathbb{C}^{KN_{RF} \times N_{RF}}$ where $\mathbf{t}_l = [t_{l,1}, t_{l,2}, \cdots, t_{l,K}]^T \in \mathbb{C}^{K \times 1}$ denotes the time delays realized by K TTDs for the l-th path. $\mathbf{F}_{BB} \in \mathbb{C}^{N_{RF} \times N_s}$ is the digital beamformer.

2.2 Communication Model

The received symbol signal of the u-th user at the m-th subcarrier at the downlink users can be given as

$$\mathbf{y}_{u,m} = \mathbf{H}_{u,m}\mathbf{X}_{u,m}\mathbf{s}_{u,m} + \mathbf{n}_{u,m} \tag{2}$$

where $\mathbf{H}_{u,m}$ is the channel matrix of the u-th user at the m-th subcarrier, $\mathbf{X}_{u,m}$ is the (u,m)-th entry of $\mathbf{X}$. $\mathbf{s}_{u,m}$ is the transmitted signal of the u-th user at the m-th subcarrier and $\mathbf{n}_{u,m}$ following Gaussian distribution $\mathcal{CN}(0, \sigma^2\mathbf{I}_{N_s})$ with σ^2 being the noise power.

Given the modulation matrix $\mathbf{S}_{u,m}$ of the u-th user at m-th subcarrier which achieve the expectation, the received signal of the u-th user at m-th subcarrier is expressed as

$$\mathbf{y}_{u,m} = \mathbf{S}_{u,m}\mathbf{s}_{u,m} + (\mathbf{H}_{u,m}\mathbf{X}_{u,m} - \mathbf{S}_{u,m})\mathbf{s}_m + \mathbf{n}_{u,m}. \tag{3}$$

The spectrum efficiency (SE) of users can be given as

$$SE = \frac{1}{M}\sum_{m=1}^{M}\sum_{u=1}^{N_s}\log(1 + SINR_{u,m}), \tag{4}$$

$$SINR_{u,m} = \frac{\mathbb{E}(|\ \mathbf{S}_{u,m}\ |^2)}{\mathbb{E}(|\ \mathbf{H}_{u,m}\mathbf{X}_{u,m} - \mathbf{S}_{u,m}\ |^2) + \mathbb{E}(\mathbf{n}_{u,m})}, \tag{5}$$

where $\mathbb{E}$ denotes the ensemble average with respect to the time index. So in order to get maximum SE, We should minimizing $\|\ \mathbf{HX} - \mathbf{S}\ \|$.

2.3 Radar Model

Denote the optimal solution obtained from omnidirectional or directional beam pattern design as $\mathbf{X}_0$. For wideband radar, SSME between the design spectrum and the expected spectrum should be minimized in order to ensure the radar performance.

$$SSME = \|\ \mathbf{X} - \mathbf{X}_0\ \|_F^2 \tag{6}$$

3. Delay-Phase Tradeoff Algorithm

The hybrid precoding problem for the OFDM-DFRC system is formulated as

$$\begin{aligned} \min_{\mathbf{X}} \quad & \rho\|\mathbf{HX} - \mathbf{S}\|_F^2 + (1-\rho)\|\mathbf{X} - \mathbf{X}_0\|_F^2 \\ \text{s.t.} \quad & \|\mathbf{X}\|_F^2 = P_T, \end{aligned} \tag{7}$$

where P_T is the total transmit power, $0 \le \rho \le 1$ is a weighting factor that determines the weights performance in the DFRC system.

The two Frobenius norms in the objective function can be combined in the form

$$\begin{aligned} & \rho\|\mathbf{HX} - \mathbf{S}\|_F^2 + (1-\rho)\|\mathbf{X} - \mathbf{X}_0\|_F^2 \\ = & \left\| \left[\sqrt{\rho}\mathbf{H}^T, \sqrt{1-\rho}\mathbf{I}_{N_t}\right]^T \mathbf{X} - \left[\sqrt{\rho}\mathbf{S}^T, \sqrt{1-\rho}\mathbf{X}_0^T\right]^T \right\|_F^2, \end{aligned} \tag{8}$$

where $\mathbf{I}_{N_t}$ denotes the $N_t \times N_t$ identity matrix. Denote $\mathbf{P} = [\sqrt{\rho}\mathbf{H}^T, \sqrt{1-\rho}\mathbf{I}_{N_t}]^T \in \mathbb{C}^{(N_s+N_t)\times N_t}$, $\mathbf{Q} = [\sqrt{\rho}\mathbf{S}^T, \mathbf{X}_0^T]^T \in \mathbb{C}^{(N_s+N_t)\times 1}$, problem (8) can be written compactly as

$$\min_{\mathbf{X}} \|\mathbf{PX} - \mathbf{Q}\|_F^2 \qquad \text{s.t.} \|\mathbf{X}\|_F^2 = P_T. \tag{9}$$

To solve this convex optimal problem as (9), the consensus-ADMM algorithm is employed. Let $\mathbf{G}(\mathbf{X}) = \|\mathbf{PX} - \mathbf{Q}\|_F^2$, the problem is simplified as

$$\min_{\mathbf{X}} \mathbf{G}(\mathbf{X}) \qquad \text{s.t. } \|\mathbf{X}\|_F^2 = P_T. \tag{10}$$

The augmenting the Lagrange function is

$$\mathcal{L}(\mathbf{X}, \mathbf{Z}, \mathbf{V}) = \mathbf{G}(\mathbf{X}) + \mathbf{V}^T(\mathbf{X} - \mathbf{Z}) + \frac{c}{2}\|\mathbf{X} - \mathbf{Z}\|, \tag{11}$$

where $\mathbf{Z}$ is the solution of $\|\mathbf{X}\|_F^2 = P_T$. Therefore, at the $(k+1)$-th iteration, the corresponding consensus-ADMM algorithm [8] framework takes the following iterations:

$$1.\mathbf{X}_i^{k+1} = \arg\min_{\mathbf{X_i}} \sum_{i=1}^{n}\mathbf{G}_i(\mathbf{X_i}) + \frac{c}{2}\sum_{i=1}^{n}\|\mathbf{X}_i - \mathbf{Z}^k + \frac{\mathbf{V}_i^k}{c}\|_2^2, \tag{12}$$

$$2.\mathbf{Z}^{k+1} = \arg\min_{\mathbf{X_i}} \frac{c}{2} \sum_{i=1}^{n} \|\mathbf{Z} - \mathbf{X}_i^{k+1} - \frac{\mathbf{V}_i f}{c}\|_2^2, \tag{13}$$

$$3.\mathbf{V}_i^{k+1} = \mathbf{V}^k + c(\mathbf{X}_i^{k+1} - \mathbf{Z}^{k+1}). \tag{14}$$

Equations (12) to (14) are repeated until a certain termination condition is met. Then the solution $\mathbf{X}_{opt}$ is addressed.

Then $\mathbf{X}_{opt}$ is used to invert the digital precoding design as follows. The phase shift values of the adjacent TTDs are equal, so the time delay vector $\mathbf{t}_l$ should satisfy $\mathbf{t}_l = [0, s_l T_c, 2 s_l T_c, \cdots, (K-1) s_l T_c]^T$, where T_c is the period of the carrier frequency f_c, and s_l denotes the number of periods that should be delayed for the l-th path component. Thus, s_l satisfies

$$-2\pi f_m s_l T_c = -\pi \alpha_{l,m}. \tag{15}$$

Substituting $T_c = \frac{1}{f_c}, \xi_m = \frac{f_m}{f_c}$ and $\alpha_{l,m} = (\xi_m - 1) P \theta_l$ into (16), we get

$$s_l = \frac{(\xi_m - 1) P \theta_l}{2 \xi_m}. \tag{16}$$

Note that in (17), the number of periods s_l is determined by not only the fixed P and the target physical orientation θ_l, but also the variable relative frequency ξ_m. This makes (17) difficult to implement for all M subcarriers, since s_l must be fixed due to the hardware constraint of TTDs. To solve this problem, we divide the phase shift $-\pi \alpha_{l,m} = -\pi(\xi_m - 1) P \theta_l$ into two parts $-\pi \xi_m P \theta_l$ and $\pi P \theta_l$.

The first frequency-dependent part can be realized by TTDs with

$$s_l = \frac{P \theta_l}{2}. \tag{17}$$

The second frequency-independent phase shift part to generate a beam aligned with the target physical direction θ_l as step 4.

$$\left[\bar{\mathbf{f}}_{l,1}^T, \cdots, \bar{\mathbf{f}}_{l,K}^T\right]^T = \left[\mathbf{a}_t(\theta_l)_{[1:P]}, e^{j\pi P \theta_l} \mathbf{a}_t(\theta_l)_{[P+1:2P]} \cdots, e^{j\pi(K-1)P\theta_l} \mathbf{a}_t(\theta_l)_{[(K-1)P+1:N_t]}\right], \tag{18}$$

where $\mathbf{f}_{l,k}, k = 1, 2, \cdots, K$ is the phase shifts provided by PSs and $\mathbf{a}_t(\theta_l)$ is the array responses at the base sation side for the l-th path. For each path component, the analog beamformer $\mathbf{F}_{RF,l}$ is calculated in step 5.

The time delays delayed by K TTDs are generated in steps 6-7. Considering the time delays $t_{l,k}$ be larger than 0, a small modification is required to be operated on (18). Finally, the time delay of the k-th delayer $t_{l,k}$ should be

$$t_{l,k} = \begin{cases} (K-1)\left|\frac{P\theta_l}{2}\right| T_c + k\frac{P\theta_l}{2} T_c, \theta_l < 0, \\ k\frac{P\theta_l}{2} T_c, \theta_l \geq 0, \end{cases} \tag{19}$$

For each subcarrier frequency, the analog beamformer $\mathbf{F}_{RF,m}^{TTD}$ is generated in step 11. Finally, the digital precoder

Algorithm 1 Delay-phase tradeoff solution

Inputs: $\mathbf{H}, \mathbf{S}, \mathbf{X_0}$,weighting factor $0 \leq \rho \leq 1$, P_T, physical direction θ_l

1: set $k = 1$, compute $\mathbf{G} = \|\mathbf{PX} - \mathbf{Q}\|_F^2$.

2: **do** equations (12-15), upadate $k : += 1$ **until** find $\mathbf{X}_{opt}$

3: **for** $l \in \{1, 2, \cdots, N_{RF}\}$ **do**

4: $\left[\bar{\mathbf{f}}_{l,1}^T, \cdots, \bar{\mathbf{f}}_{l,K}^T\right]^T = \left[\mathbf{a}_t(\theta_l)_{[1:P]}, e^{j\pi P\theta_l} \mathbf{a}_t(\theta_l)_{[P+1:2P]}, \cdots, e^{j\pi(K-1)P\theta_l} \mathbf{a}_t(\theta_l)_{[(K-1)P+1:N_t]}\right]$

5: $\mathbf{F}_{RF,l}$ =blkdiag $\left(\left[\bar{\mathbf{f}}_{l,1}, \cdots, \bar{\mathbf{f}}_{l,K}\right]\right)$

6: $t_{l,k} = \begin{cases} (K-1)\left|\frac{P\theta_l}{2}\right| T_c + k\frac{P\theta_l}{2} T_c, \theta_l < 0, \\ k\frac{P\theta_l}{2} T_c, \theta_l \geq 0, \end{cases}$

7: $\mathbf{t}_l = \left(\left[t_{l,1}, \cdots, t_{l,K}\right]\right)^T$

8: **end for**

9: $\mathbf{F}_{RF} = \left[\mathbf{F}_{RF,1}, \mathbf{F}_{RF,2}, \cdots, \mathbf{F}_{RF,N_{RF}}\right]$

10: **for** m $\in \{1, 2, \cdots, M\}$ **do**

11: $\mathbf{F}_{RF,m}^{TTD}$=blkdiag $\left(\left[e^{-j2\pi f_m \mathbf{t}_1}, \cdots, e^{-j2\pi f_m \mathbf{t}_{N_{RF}}}\right]\right)$

12: $\mathbf{X}_{m,eq} = \mathbf{X}_{opt,m}^H \mathbf{F}_{RF,m} \mathbf{F}_{RF,m}^{TTD}$

13: $\mathbf{F}_{BB,m} = \mu \mathbf{V}_{m,eq,[:,1:N_{RF}]}$, $\mathbf{X}_{m,eq} = \mathbf{U}_{m,eq} \mathbf{\Sigma}_{m,eq} \mathbf{V}_{m,eq}^H$

14: **end for**

Output: $\mathbf{F}_{RF,m}, \mathbf{F}_{RF,m}^{TTD}, \mathbf{F}_{BB,m}$

$\mathbf{F}_{BB}$ is calculated based on singular value decomposition (SVD) precoding in steps 12-13 where μ is the power normalization coefficient. Utilizing the ordered SVD of $\mathbf{X}_{opt,m}$ as

$$\mathbf{X}_{opt,m} = \mathbf{U}_m \Sigma_m^f \mathbf{V}_m^H, \tag{20}$$

where the diagonal matrix Σ_m^f=diag$([\lambda_1, \lambda_2, \cdots, \lambda_{d_m}]) \in \mathbb{C}^{d_m \times d_m}(\lambda_i, i{=}1{,}2{,}\cdots, d_m)$ representing the singular value of $\mathbf{X}_{opt,m}$, the matrix $\mathbf{V}_m^f \in \mathbb{C}^{N_t \times d_m}$ with $\mathbf{V}_m^{fH} \mathbf{V}_m^f = \mathbf{I}_{d_m}$ are obtained from the ordered SVD of the channel $\mathbf{X}_{opt,m}$, where d_m denotes the rank of $\mathbf{X}_{opt,m}$. For clarity, we summarize the above approach in Algorithm 1.

4. Simulations and Result

We use a Monte-Carlo simulation to verify the performance of delay-phase tradeoff algorithm with the widely used wideband raybased channel model [9] for THz communications. We set $P_T = 1, M = 64, N_s = 4, K = 16$ and each entry of the channel matrix $\mathbf{H}$ subject to standard Complex Gaussian distribution. We employ $N_{RF} = 4$ RF chains and $N_t = 256$ antennas ULA. The constellation chosen for the communication users is the unit-power QPSK alphabet. Note that the required number of TTDs K in the proposed delay-phase tradeoff structure must be much smaller than antennas number N_t. The hybrid DFRC precoding [10], the wideband hybrid DFRC precoding [11] and spatially sparse DFRC precoding [12] are employed to compare under the radar performance constraint.

Figure 2 compares the average achievable rate in DFRC system with different SNR. It is found that other schemes such as space sparse precoding suffer great loss of communication performance because wideband hybrid beamforming will cause beam splitting, but the delay-phase DFRC precoding method can adjust the beam direction to solve this

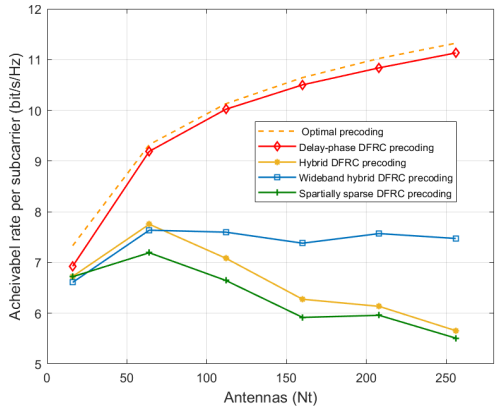

Fig. 2 Achievable rate performance about antennas number N_t.

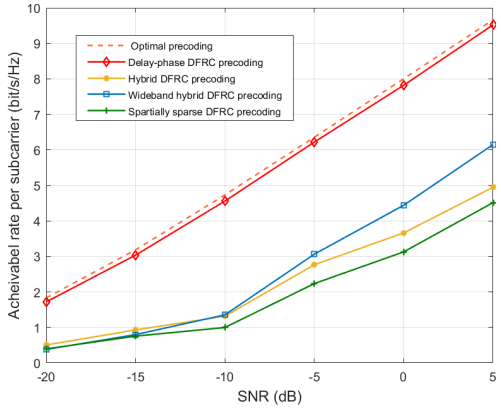

Fig. 3 Achievable rate performance about SNR.

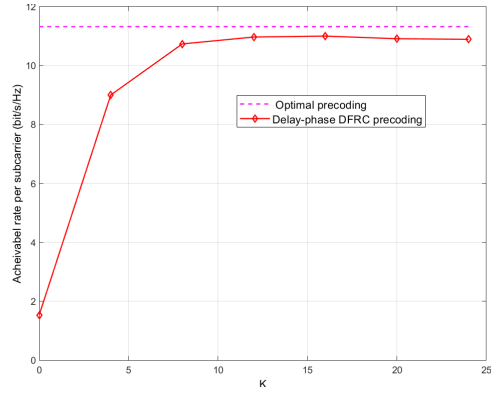

Fig. 4 Achievable rate performance about K.

problem and get higher efficiency. Figure 3 contrasts the average achievable rate in DFRC system with different antennas number. It is obtained that as the increase of antennas number, the communication performance difference between the delay phase tradeoff precoding method and other methods is increasing. Figure 4 expressed the communication performance with K true-time-delayers. As the increase of TTDs number, the beam split effect is better overcamed.

5. Conclusion

In this letter, we discuss the hybrid beamforming precoding of wideband DFRC system, which can be used for both target detection and downlink communications. We apply a delay phase tradeoff precoding method. Specifically, we obtain its global optimal fully digital precoding based on the consensus-ADMM framework. Then the delay phase precoding method is used to invert the digital precoding design schemes. The simulation results show that this proposed beamforming precoding method has significant array gain between radar and communication, and higher adaptability for large antennas number scenarios.

References

[1] F. Liu, C. Masouros, A.P. Petropulu, H. Griffiths, and L. Hanzo, "Joint radar and communication design: Applications, state-of-the-art, and the road ahead," IEEE Trans. Commun., vol.68, no.6, pp.3834–3862, 2020.

[2] F. Liu, C. Masouros, A. Li, H. Sun, and L. Hanzo, "MU-MIMO communications with MIMO radar: From co-existence to joint transmission," IEEE Trans. Wireless Commun., vol.17, no.4, pp.2755–2770, 2018.

[3] X. Liu, T. Huang, N. Shlezinger, Y. Liu, J. Zhou, and Y.C. Eldar, "Joint transmit beamforming for multiuser MIMO communications and mimo radar," IEEE Trans. Signal Process., vol.68, pp.3929–3944, 2020.

[4] M.F. Keskin, V. Koivunen, and H. Wymeersch, "Limited feedforward waveform design for OFDM dual-functional radar-communications," IEEE Trans. Signal Process., vol.69, pp.2955–2970, 2021.

[5] Z. Cheng, Z. He, and B. Liao, "Hybrid beamforming design for OFDM dual-function radar-communication system," IEEE J. Sel. Topics Signal Process., vol.15, no.6, pp.1455–1467, 2021.

[6] Z. Xu and A. Petropulu, "A wideband dual function radar communication system with sparse array and OFDM waveforms," arXiv preprint, arXiv: 2106.05878, 2021.

[7] J. Tan and L. Dai, "Delay-phase precoding for THz massive MIMO with beam split," Proc. IEEE Global Commun. Conf. (IEEE GLOBECOM'19), pp.1–6, 2019.

[8] S. Boyd, N. Parikh, E. Chu, B. Peleato, and J. Eckstein, "Distributed optimization and statistical learning via the alternating direction method of multipliers," Found. Trends Mach. Learn., vol.3, no.1, pp.1–122, 2011.

[9] B. Peng, K. Guan, and T. Kurner, "Cooperative dynamic angle of arrival estimation considering space-time correlations for terahertz communications," IEEE Trans. Wireless Commun., vol.17, no.9, pp.6029–6041, Sept. 2018.

[10] S. Park, A. Alkhateeb, and R.W. Heath, Jr., "Dynamic subarrays for hybrid precoding in wideband mmWave MIMO systems," IEEE Trans. Wireless Commun., vol.16, no.5, pp.2907–2920, 2017.

[11] X. Liu and D. Qiao, "Space-time block coding-based beamforming for beam squint compensation," IEEE Wireless Commun. Lett., vol.8, no.1, pp.241–244, 2019.

[12] O. El Ayach, S. Rajagopal, S. Abu-Surra, Z. Pi, and R.W. Heath, Jr., "Spatially sparse precoding in millimeter wave MIMO systems," IEEE Trans. Wireless Commun., vol.13, no.3, pp.1499–1513, 2014.